THE JOURNAL OF BIOLOGICAL CHEMISTRY
Vol. 273, No. 12, Issue of March 20, pp. 7052–7058, 1998

Printed in U.S.A.

Enhancement of ATP Levels and Glucose Metabolism during an Infection by *Chlamydia*

NMR STUDIES OF LIVING CELLS*

(Received for publication, December 15, 1997, and in revised form, January 7, 1998)

David M. Ojcius‡, Hadassa Degani§, Joel Mispelter¶, and Alice Dautry-Varsat

From the Unité de Biologie des Interactions Cellulaires, CNRS 1960, Institut Pasteur, Paris, France and the ¶Institut Curie, INSERM U350, Orsay, France

The *Chlamydia* species are obligate intracellular bacteria that proliferate only within the infected cell. Since the extracellular bacteria are metabolically inert and there are no cell-free systems for characterizing *Chlamydia* metabolism, we studied metabolic changes related to ATP synthesis and glycolysis in HeLa cells infected with *Chlamydia psittaci* during the course of the 2-day infection cycle using noninvasive ^{31}P and ^{13}C NMR methods. We find that the infection stimulates ATP synthesis in the infected cell, with a peak of ATP levels occurring midway through the infection cycle, when most of the metabolically active bacteria are proliferating. The infection also stimulates synthesis of glutamate with a similar time course as for ATP. The stimulation is apparently due to an enhancement in glucose consumption by the infected cell, which also results in an increased rate of lactate production and glutamate synthesis as well as higher glycogen accumulation during the infection. Concurrently, infection leads to an increase in the expression of the glucose transporter, GLUT-1, on HeLa cells, which may account for the enhanced glucose consumption. The chlamydiae are thus able to stimulate glucose transport in the host cell sufficiently to compensate for the extra energy load on the cell represented by the infection.

Chlamydia species are causative agents of conjunctivitis and pneumonia, and they are recognized as the leading cause of bacterially acquired sexually transmitted infections. On repeated exposure, the consequences can be blinding trachoma or sequelae from sexually transmitted infection, such as epididymitis or pelvic inflammatory diseases, ectopic pregnancy, or tubal infertility (1, 2). Despite the clinical importance of these infections, the biology and biochemistry of *Chlamydia* infection remains poorly understood.

The chlamydiae are obligate intracellular bacteria that proliferate only within the infected host cell. In line with its requirement for host cell metabolites for survival, *Chlamydia* exists in two developmental states, elementary bodies (EBs)[1] and reticulate bodies (RBs). EBs represent the metabolically inactive, infectious form of the bacteria, and they are internalized into host cells within membrane-bound vacuoles that avoid fusion with host-cell lysosomes (3). Within 6–10 h after internalization, the EBs differentiate into the metabolically active RBs. This transformation triggers DNA, RNA, and protein synthesis in the RBs, which proliferate in the growing vacuole and produce up to a thousand progeny. Lipids from the *trans*-Golgi network are transported to this membrane (4), and the bacteria contribute their own proteins to the inclusion membrane (5). An intimate association thus exists between the bacteria and the host, but the lack of molecular tools in the field has made further characterization of the association difficult. After approximately 2 days of infection, RBs differentiate back into EBs, and a new infection cycle can begin.

Chlamydia trachomatis grows well in cytoplasts (enucleated cells) (6), indicating that active host cell nuclear function is not required for bacterial growth. In addition, bacteria grow in host cells treated with certain protein synthesis inhibitors, implying that *de novo* protein synthesis by the host cell is also not required (7). Nonetheless, a cell-free system for *Chlamydia* has never been obtained (3), and host-free RBs have limited metabolic activity (8). The metabolism of the bacteria must therefore be studied in infected cells themselves.

We have addressed metabolic changes in the infected cell using a non-invasive NMR technique that allowed us to measure the levels and rates of production of a number of metabolites related to energy metabolism, including ATP, glucose, lactate, and glutamate. We find a marked enhancement in the levels of the energy metabolites that correlates well with the infection cycle of *Chlamydia*. Concomitantly with this enhancement, glucose consumption, lactate production, glutamate synthesis via the tricarboxylic acid cycle, and glucose incorporation into glycogen increase, apparently due to increased surface expression of glucose transporters by the host cell. The chlamydiae thus fulfill their energy requirements by increasing the expression of host cell glucose transporters, which by itself could account for the other changes that we observe in energy-metabolite levels.

EXPERIMENTAL PROCEDURES

Cells and Materials—The *Chlamydia* species used here, the guinea pig inclusion conjunctivitis serovar of *Chlamydia psittaci* has been described elsewhere (9). HeLa cells were maintained in a humidified incubator at 37 °C with 5% CO_2 in high glucose Dulbecco's modified Eagle's medium (Life Technologies, Inc.) supplemented with 10% heat-inactivated fetal calf serum, 2 mM L-glutamine, and 50 μg/ml gentamicin. The rabbit polyclonal antibody against the carboxyl terminus of GLUT-1 (AB1340) was from Chemicon (Euromedex, Strasbourg, France), and the fluorescein isothiocyanate-labeled anti-*Chlamydia* lipopolysaccharide monoclonal antibody (clone C4) was from Argene (Varilhes, France). *R*-Phycoerythrin-conjugated goat anti-rabbit IgG was from Molecular Probes (Eugene, OR). Uridine 5′-diphospho-*N*-acetylglucosamine, uridine 5′-diphosphoglucoronic acid, and uridine

* This work was supported by the Institut Pasteur, CNRS, Institut Curie (Orsay), and an EMBO fellowship (to H. D.). The costs of publication of this article were defrayed in part by the payment of page charges. This article must therefore be hereby marked "*advertisement*" in accordance with 18 U.S.C. Section 1734 solely to indicate this fact.

‡ To whom correspondence should be addressed: Institut Pasteur, Biologie des Interactions Cellulaires, 25 rue du Dr. Roux, 75724 Paris Cedex 15, France. Tel.: 33-1-40-61-30-64; Fax: 33-1-40-61-32-38; E-mail: ojcius@pasteur.fr.

§ Permanent address: Dept. of Biological Regulation, The Weizmann Institute of Science, Rehovot, Israel.

[1] The abbreviations used are: EB, elementary body; RB, reticulate body; UDPS, uridine diphosphate sugars; PBS, phosphate-buffered saline; m.o.i., multiplicity of infection.

5′-diphosphoglucose were from Sigma.

Preparation of Chlamydiae—The chlamydiae were grown in infected HeLa cell monolayer cultures essentially as described (10). Briefly, infected HeLa cells were cultured on 20 9-cm Petri culture dishes and harvested at 48 h postinfection. The cells and supernatant were combined and centrifuged for 60 min at 12,000 rpm in a Sorvall type GSA rotor. The pellet was resuspended in ice-cold sucrose/phosphate/glucose buffer (SPG), and the cells were sonicated on ice for 30 s. The resulting suspension was centrifuged for 10 min at 2,000 rpm in a Sorvall SS34 rotor to remove unbroken cells, and the new supernatant was centrifuged again for 30 min at 15,000 rpm at 4 °C to collect the bacteria. The pellet was resuspended in ice-cold SPG with a 21-gauge 2-ml syringe to dissociate aggregates, giving the final suspension of EBs used in subsequent infection experiments. This suspension was aliquoted and stored at −80 °C until ready for use.

Cell Cultures on Beads—HeLa cells cultivated in a standard manner were trypsinized and seeded on 150-μm biosylon microspheres (Nunc, Denmark) or 300-μm polyacrolein microspheres (11) in small, sterile plastic vials (3 million cells per 0.5-ml beads in 4 ml of standard growth medium described above). The vials were placed in the incubator (37 °C, 5% CO_2, humidified) and agitated gently every 15 min for a duration of 3 h. The beads with cells were then transferred to 9-cm bacteriological Petri dishes and additional medium was added until 12 ml was reached. Medium was replaced every 2 days. Before the NMR experiment, the beads were collected (2- or 2.5-ml beads) and transferred to a sterile 10-mm NMR tube. The tube was then placed in the NMR spectrometer and perfused with oxygenated growth medium at 37 °C using a sterile perfusion system described in detail elsewhere (12).

For NMR experiments using *Chlamydia*-infected cells, biosylon beads preseeded 2 days before with HeLa cells were incubated with *C. psittaci* at (0.5-ml beads/2 ml of medium) at a multiplicity of infection (m.o.i.) of approximately 0.3, and left on an agitator for 1 h before adding additional culture medium (12 to 0.5 ml beads). Two to 2.5 ml of infected HeLa cells on beads were transferred to a sterile NMR tube, and perfusion and data acquisition was performed as for the uninfected HeLa cells.

For cell growth studies, HeLa cells were grown and infected on beads as for NMR experiments (m.o.i. = ~0.3). Infected and uninfected cells were trypsinized at the indicated times and counted using the viability trypan blue exclusion method and light microscopy. In a separate experiment, uninfected cells and cells infected with an m.o.i. of ~1.0 were harvested and viable cells were identified by their ability to exclude propidium iodide in a FACScan flow cytometer (Becton Dickinson, San Jose, CA).

Electron Microscopy—Cells cultured on agarose-polyacrolein beads were infected with chlamydiae for 0, 24, or 45 h and were fixed with 2.5% glutaraldehyde overnight at 4 °C. The fixed cells were centrifuged twice for 20 min at 15,000 rpm in PBS, and the pellet was transferred in 2 ml of cacodylate buffer (5 mM $CaCl_2$, 5 mM $MgCl_2$, 0.2 M cacodylate, pH 7) into an Eppendorf tube. The tube was centrifuged and the pellet was resuspended in 200 μl of 3% agar (Difco) in cacodylate buffer at 45 °C. The warm agar was centrifuged 1 min at 15,000 rpm and then allowed to solidify at 4 °C. One ml of 1% OsO_4 in cacodylate buffer was added to the agar, and after leaving for 1 h at room temperature, the supernatant was removed and the pellet was incubated in a 1% uranyl acetate (Merck) solution in cacodylate buffer for another hour at room temperature. The supernatant was removed, the pellet was rinsed with water and then dehydrated by rinsing with increasing concentrations (25, 50, 75, and 100%) of acetone. The preparations were then embedded in Epon. Ultra-thin sections (60 μm) were prepared on an Ultra Cut 2 Reichert GUNG microtome and poststained with uranyl acetate and lead citrate for examination on a Zeiss electron microscope at an accelerating voltage of 50 kV.

NMR Spectroscopy and Data Analysis—Approximately 2–2.5 ml of beads with about 1–2 × 10^7 cells were introduced to the NMR probe in each experiment and were perfused with 60–400 ml of medium, depending on the length and conditions of the experiment.

NMR recording was performed with a Unity 400 spectrometer (Varian). The temperature in the probe was maintained constant at 37 °C (in the sample). ^{31}P spectra were recorded at 161 MHz using 45° pulses, an acquisition time of 0.2 s, and a repetition time of 2 s without proton decoupling. Each spectrum consisted of 1800 transients accumulated in 60 min. The chemical shifts of the ^{31}P signals were assigned in reference to α-NTP at −10.03 ppm. Since the line widths of the signals did not alter throughout the course of the experiment, changes in signal intensity were directly proportional to changes in the concentrations of the metabolite.

^{13}C spectra were recorded at 100 MHz by applying 45° pulses, with 1-s repetition time and composite pulse proton decoupling during acquisition of ~2 watt. During the relaxation delay, the decoupling power was reduced 60-fold. Each spectrum was acquired for 30 min (1800 transients). These spectra were used to follow the energetics of the HeLa cells through glycolysis, as well as monitoring the rates of glucose consumption and lactate production and incorporation of the label into glycogen and glutamate. For these measurements, glucose-free Dulbecco's modified Eagle's medium supplemented with 11.2 or 16.8 mM [1-^{13}C]glucose (99% enriched, from Cambridge Isotope Laboratories, Andover, MA) in 100–150 ml of re-circulating medium was used. The ^{13}C signal of C1-β-glucose (96.8 ppm) served as a reference for chemical shift determination. The rate of glucose utilization was determined from the decrease in the [1-(^{13}Cα + ^{13}Cβ)]glucose intensity and the rate of lactate synthesis was measured from the increase in the [3-^{13}C]lactate signal at 21 ppm. The rates of labeling of C-4 glutamate and C-1 glucose moieties in glycogen were determined from the change in the corresponding signal intensities (at 32.4 and 101.4 ppm, respectively).

Preparation of Cell Extracts for NMR Spectroscopy—Water-soluble metabolites from HeLa cells were extracted as described previously (13). Briefly, cells were extracted with methanol, chloroform, and water (1:1:1, v/v/v), and the contents of the chloroform and methanol/water phases were separated and recovered. ^{31}P spectra of the water-soluble metabolites were obtained with a Unity 500 spectrometer (Varian) at a temperature of 25 °C. The spectra were recorded at 202 MHz using 45° pulses and a repetition time of 2.9 s with proton decoupling.

Cytofluorimetry Measurement of GLUT-1 Expression—Adherent HeLa cells growing at 50% confluence on 75-cm^2 tissue culture flasks (Costar) were incubated with 2 ml of chlamydiae (m.o.i. = ~0.3) or PBS for 2 h, agitating gently every 15 min, after which 10 ml of culture medium was added. After culture for 1 day, the cells were detached with EDTA, resuspended in 10 ml of PBS, and centrifuged at 1,200 rpm for 5 min. The supernatant was removed and the pellet was fixed by resuspending in 1 ml of 3.7% paraformaldehyde and neutralizing with 50 mM NH_4Cl as described previously (14). Following two additional washes with PBS, the cells were incubated in 100 μl with the fluorescein isothiocyanate-labeled anti-*Chlamydia* monoclonal antibody (1:100 dilution) and the rabbit polyclonal anti-GLUT-1 antibody (1:100 dilution) in PBS containing 0.05% saponin for 45 min at 4 °C. The cells were washed and incubated with 100 μl of the phycoerythrin-conjugated goat anti-rabbit IgG (10 μg/ml) in PBS, 0.05% saponin for another 30 min at 4 °C. Finally, the cells were washed twice in PBS without detergent, resuspended in 1 ml of PBS/bovine serum albumin, and transferred into 12 × 75-mm Falcon® 2052 FACS tubes (Becton Dickinson, San Jose, CA). Data from 10,000 HeLa cells were collected on the FACScan flow cytometer with an argon-ion laser tuned to 488 nm, and the mean fluorescence intensity was obtained from the recorded data.

RESULTS

Growth and Infection of HeLa Cells on Beads—Mammalian cells growing on biosylon and polyacrolein microspheres have previously been used for non-invasive NMR measurements (11), and *C. trachomatis* has likewise been used to infect McCoy cells and HEC-1B cells growing on beads (15, 16). We therefore verified whether *C. psittaci* could infect bead-bound HeLa cells under the conditions of our NMR experiments. The density of uninfected HeLa cells was first evaluated by low magnification light microscopy, which revealed predominantly a monolayer of HeLa cells growing at near confluence under the conditions used for NMR (Fig. 1*A*). Electron microscopy showed that uninfected HeLa cells were bound to the beads (Fig. 1*B*). After a 45-h infection with chlamydiae, a large inclusion containing bacteria at both the EB and RB developmental stages is readily apparent (Fig. 1*C*), while the host cell still remains firmly attached to the bead.

Effects of Chlamydia Infection on HeLa Cell Growth—The NMR signal for most of the metabolites measured below is derived only from living HeLa cells, which can retain these metabolites; dead cells are spectroscopically silent since the metabolites leaking from dead cells are diluted in the extracellular perfusion medium. To assess the viability and growth rate of cells on beads, we therefore studied the growth curves for HeLa cells growing on beads that have been infected with *C. psittaci* or incubated with control growth medium. The cell

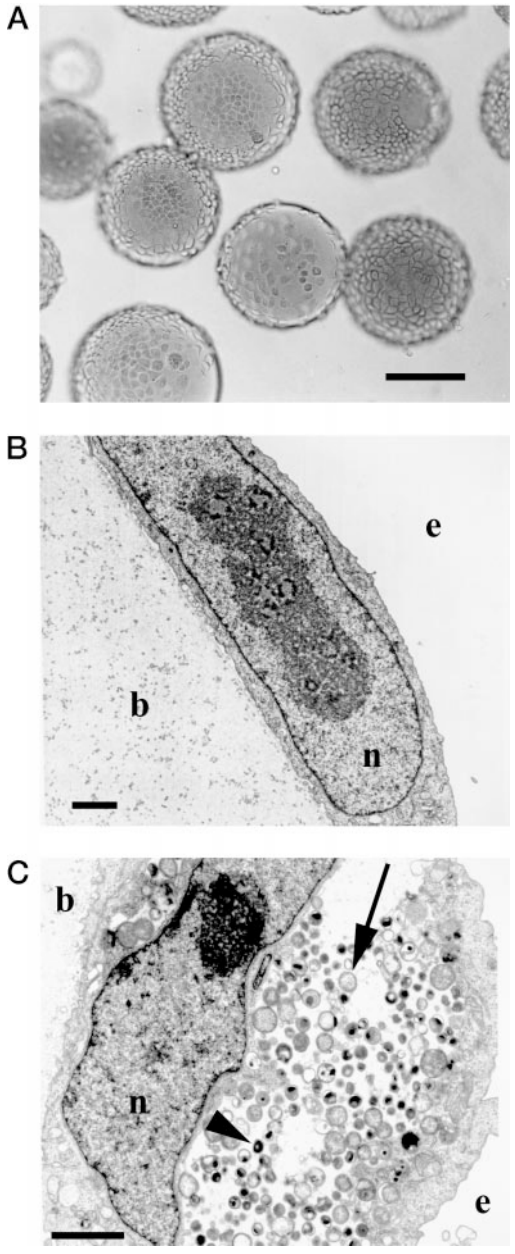

FIG. 1. **Microscopic characterization of HeLa cells growing on beads.** *A*, a low magnification profile of confluent cells on beads, visualized by conventional light microscopy. *B*, electron micrographs of uninfected cells; and *C*, cells infected with *C. psittaci* for 45 h, showing the beads (*b*), host cell nucleus (*n*), and extracellular space (*e*). The *arrowhead* points to a typical *C. psittaci* EB, and the *arrow* points to an RB. *Scale bars*, 100 μm (*A*), 2 μm (*B*), and 2 μm (*C*).

number on beads was also counted in parallel to the NMR experiments. An average of the growth curves for several NMR experiments ($n = 4$ for infected cells, $n = 5$ for control uninfected cells) is shown in Fig. 2, which indicates that infection at the m.o.i. used here (~0.3) may have a slight effect on the number of living cells. In a separate experiment, viability was also measured using the propidium iodide exclusion assay by cytofluorimetry, using an m.o.i. of ~1.0. Under these conditions, about one-third of the cells were dead after a 2-day infection (not shown), suggesting that the small effect seen in Fig. 2 may be significant.

^{31}P NMR Spectra of HeLa Cells—Uninfected HeLa cells or HeLa cells infected with *C. psittaci* were transferred to a sterile NMR tube, and the tube was placed in the NMR spectrometer and perfused at 37 °C with oxygenated growth medium for

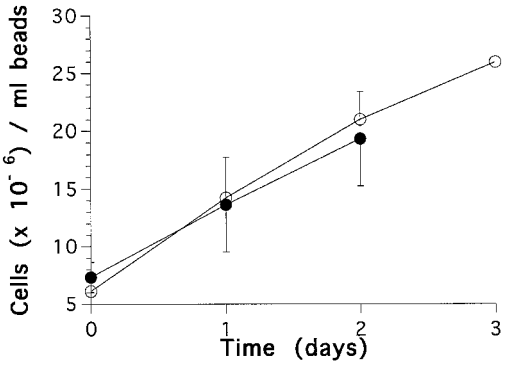

FIG. 2. **Growth curve of HeLa cells on beads.** Uninfected cells (○) or *Chlamydia*-infected cells (●) growing on beads were harvested at different times and living cells were counted, as described under "Experimental Procedures."

periods up to 3 days. Sequential ^{31}P spectra were acquired continuously and signal-averaged every hour. A full spectrum of uninfected HeLa cells on beads is shown in Fig. 3*A*. The most prominent peaks are due to phosphocholine, inorganic phosphate (P_i), the γ-phosphate of nucleoside triphosphate (γ-NTP) (which also includes β-NDP), α-NTP (which also includes α-NDP), β-NTP, and uridine diphosphate sugars (UDPS). The assignment of the peaks was based on known chemical shifts of phosphate metabolites from previous studies (17, 18), and by spiking the NMR spectra of uninfected HeLa cell extracts with uridine 5′-diphospho-*N*-acetylglucosamine, uridine 5′-diphosphoglucoronic acid, and uridine 5′-diphosphoglucose. A typical extract spectrum is shown in Fig. 3*B*, which reveals the presence of the same metabolites as in Fig. 3*A*, but also resolves the γ-NTP peak into γ-NTP and β-ADP, and the α-NTP peak into α-NTP and α-NDP. Furthermore, the peak for UDPS is resolved into UDP-*N*-acetylglucosamine, UDP-*N*-acetylgalactosamine, and UDP-glucoronic acid. However, due to the invasive nature of the extraction technique and difficulties in quantitating the energy metabolites in extracts, this technique was not used to study metabolism as a function of time during the infection.

Previous studies have determined that most of the nucleoside triphosphates consist of ATP, which typically constitutes 60–70% of the total NTP population (19, 20). In addition, the P_i peak, which is highly sensitive to the pH of the medium, is resolved in the living cells into two peaks, corresponding to the extracellular pH of the growth medium and the intracellular host cell pH (Fig. 3*A*). The peak due to the intracellular pH remains as a single peak during the entire course of infection (not shown), implying that the pH of the vacuole containing chlamydiae, from early internalization time points through the development of RB-laden inclusions, does not differ significantly from the cytosolic pH, or that the amount of P_i in the vacuole is too low to be detected by this technique. This agrees with previous immunofluorescence studies with pH-sensitive dyes showing that the pH of the *Chlamydia* vacuole is approximately neutral during the infection (21, 22).

Time Course of Phosphate Metabolite Levels during Infection—Changes in the levels of the different metabolites were determined as a function of time by measuring the intensity of each peak in spectra recorded sequentially. As the line width of each peak did not vary during the NMR recording, changes in peak intensity are directly proportional to changes in the metabolite content. Fig. 4 shows the relative concentration for γ-ATP and β-ATP during 2 days, *i.e.* during one *Chlamydia*-infection cycle. As mentioned above, the γ-ATP peak includes a minor contribution from β-ADP, but the β-ATP peak is due solely to β-ATP. Compared with the levels in uninfected cells,

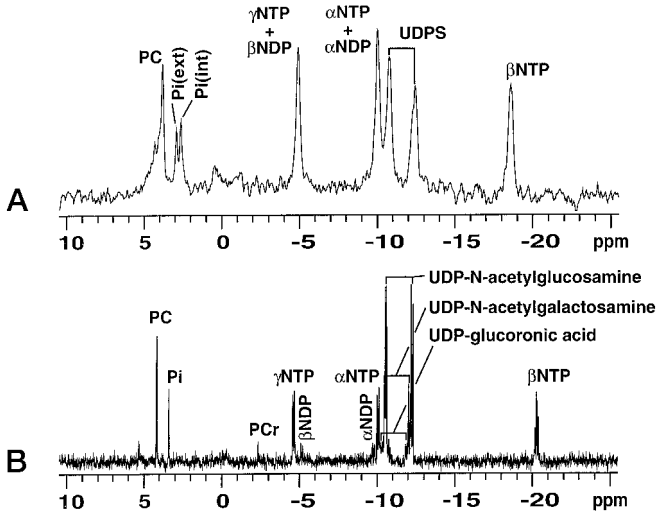

FIG. 3. **^{31}P spectra of HeLa cells.** *A*, spectrum of living cells growing on beads, acquired through noninvasive NMR as described under "Experimental Procedures." The main peaks correspond to phosphocholine (*PC*), extracellular and intracellular inorganic phosphate (P_i), γ-nucleoside triphosphate (*γ-NTP*) plus β-nucleoside diphosphate (*β-NDP*), α-NTP plus α-NDP, β-NTP, and UDPS. *B*, spectrum of water-insoluble extract, acquired with conventional NMR as described under "Experimental Procedures." Besides the peaks observed in living cells, peaks corresponding to phosphocreatine (*PCr*), UDP-*N*-acetylglucosamine, UPD-*N*-acetylgalactosamine, and UDP-glucoronic acid, as well as β-NDP and α-NDP, become apparent. The two P_i peaks in living cells collapse into one peak in the extracts.

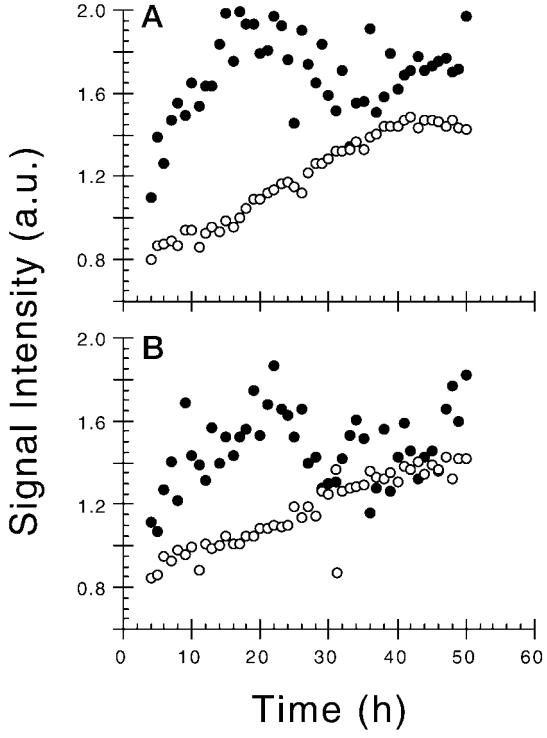

FIG. 4. **Relative concentrations of representative energy metabolites studied as a function of time by noninvasive NMR.** ^{31}P spectra were acquired in uninfected cells (○) or *Chlamydia*-infected cells (●) as described under "Experimental Procedures," and the peak intensities for (*A*) γ-ATP plus β-ADP and (*B*) β-ATP were plotted as a function of time.

which increase monotonously due to continuing cell growth in the NMR tube (see Fig. 2), there is an approximately 2-fold enhancement in the levels of γ-ATP and β-ATP in the infected cells. The signal for these metabolites was normalized at time 0 for the number of cells at the start of the NMR experiment. Since these values were not normalized for later time points, the increase in γ-ATP and β-ATP levels in infected cells may in fact be underestimated if there are fewer living cells among the infected cells than among the uninfected cells. With the exception of phosphocholine (not shown), which should not be affected appreciably by the energy requirements of the cell, all the metabolites associated with energy consumption are enhanced by infection.

For poorly understood reasons, the UPDS levels are not directly proportional to the number of cells, but can also vary as a consequence of minor changes in cell culture conditions (23). Thus, although we observed changes in UDPS levels in infected cells that paralleled the enhancement seen for ATP, we were unable to obtain reproducible changes in UDPS levels in different uninfected cell samples (not shown).

^{13}C NMR Spectra of Infected HeLa Cells—To investigate the possible origin of the ATP concentration enhancement, we also measured changes in the metabolism of glucose. ATP is produced when glucose is metabolized via glycolysis to lactate, and through the tricarboxylic acid cycle, which is coupled to oxidative phosphorylation. Besides glucose, the intermediates and end products observed by us are glycogen, lactate, and glutamate.

For these experiments, HeLa cells were transferred into the NMR tube as above, but the growth medium in the perfusion system was replaced with a medium containing [1-^{13}C]glucose at time 0. Fig. 5 displays the ^{13}C NMR spectra obtained immediately after adding the ^{13}C-labeled glucose (0 h, spectrum A) and 25 h later (spectrum B). At 0 h, the main metabolites observed are the α- and β-stereoisomers of glucose, which are predominantly in the perfusion medium, with a small broad peak around 30 ppm corresponding to the natural abundance of ^{13}C, primarily intracellular membrane components. At 25 h, there is a significant decrease in the intensity of the [1-^{13}C]glucose peaks, with a concomitant increase of other peaks, especially [3-^{13}C]lactate, which is secreted and accumulated in the perfusion medium, the intracellular [4-^{13}C]glutamate, and the [1-^{13}C]glucose residue in glycogen.

The rates for glucose consumption and lactate production were determined by plotting the intensities of the corresponding peaks and measuring the slopes from 10 consecutive spectra (equivalent to 5 h) at a time. The *insets* of Fig. 5 display representative intensity *versus* time data for glucose disappearance and lactate appearance, from which an acceleration in glucose consumption can be seen for the infected cell samples, since the glucose and lactate curves intersect sooner in the infected cell sample. Fig. 6 shows the slopes calculated for both glucose consumption and lactate production. Invariably, the rate of glucose consumption after 1 day of infection was at least twice as high as in the uninfected controls.

Glutamate and glycogen labeling could be followed in the same experiment. As opposed to glucose and lactate, which are present predominantly in the growth medium, glutamate and glycogen are present intracellularly. Similarly to the case for ATP, infection with *C. psittaci* leads to an enhancement in the rate of synthesis of glutamate, whose levels are highest midway through the infection cycle (Fig. 7*A*), and to glucose incorporation into glycogen (Fig. 7*B*). In both infected and control cells, glucose incorporation into glycogen occurs rapidly when the perfusion medium with ^{13}C-labeled glucose is introduced, but in infected cells the accumulation of labeled glycogen is about twice as high as in the uninfected controls (Fig. 7*B*).

GLUT-1 Expression in Infected HeLa Cells—The rate of glycolysis is limited by the concentration of the initial substrate, glucose, which is in turn regulated by the presence of glucose transporters on the cell surface (24–26). To determine if the

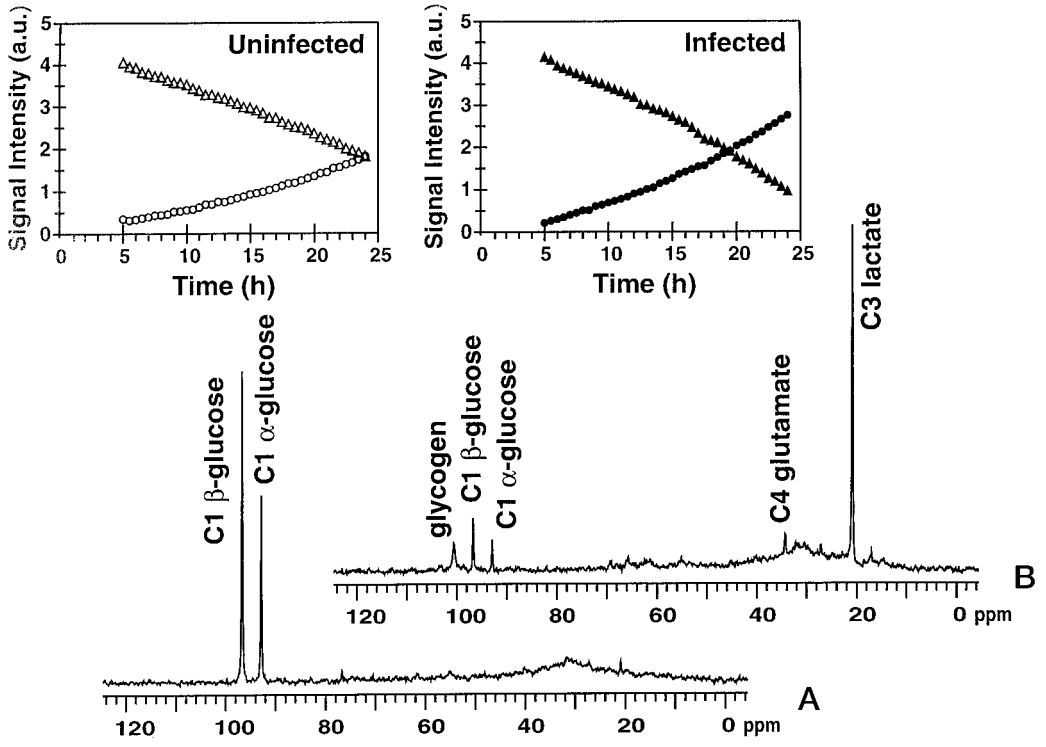

FIG. 5. **^{13}C spectra of HeLa cells.** Spectrum of living cells growing on beads, acquired immediately after the addition of ^{13}C-labeled glucose (0 h, spectrum *A*) and 25 h later (spectrum *B*). At 0 h, the main peaks correspond to the α- and β-isomers of glucose, between 90 and 100 ppm. At 30 h, there is a decrease in the intensity of the [1-^{13}C]glucose peaks, with a concomitant increase of [3-^{13}C]lactate and [4-^{13}C]glutamate, and the [1-^{13}C]glucose in glycogen. The *insets* show the intensity of the glucose (*triangles*) and lactate (*circles*) peaks as a function of time in uninfected cells (*left inset*) and cells that had been infected with *C. psittaci* at 0 h (*right inset*).

enhanced glucose consumption and lactate production, and consequently increased ATP levels, may be due to *Chlamydia*-induced up-regulation of glucose transport, we evaluated whether the expression of the ubiquitous glucose transporter, GLUT-1 (27), changes during infection.

HeLa cells were incubated with growth medium or infected with *C. psittaci* for 24 h, detached from the flasks, fixed with paraformaldehyde, and permeabilized and incubated with monoclonal antibody against *Chlamydia* and polyclonal antibodies against GLUT-1. By cytofluorimetry, it was determined that the infection caused up-regulation of GLUT-1 in the infected HeLa cell sample by a factor of 1.93 $\pm$ 0.30 (n = 4), consistent with the enhancement of glucose consumption due to infection seen by NMR.

DISCUSSION

The large number of chlamydiae that proliferate within host cells midway through infection raises the obvious question of whether the host cells and/or bacteria can synthesize an additional amount of ATP to compensate for the infection, or whether ATP levels in the host cell decrease during the infection due to the extra energetic demands of the bacteria. We find that not only is sufficient ATP synthesized in the infected cells to maintain normal metabolic levels, but that the ATP concentration increases above normal levels. A similar *Chlamydia*-induced 2–3-fold enhancement was observed for glycogen and glutamate, and their levels peaked halfway through the infection cycle (24 h), when the metabolic activity of the chlamydiae are also at their highest levels. The concentrations of the energy metabolites then decreased to near-normal levels by 48 h, when many of the RBs have begun to differentiate back to the metabolically inactive EBs. These unexpected changes were paralleled by an increase in the transport and consumption of glucose by the infected cell, which may thus account for most if not all of the extra energy metabolites. Consistent with this interpretation, it has been reported for both cell and animal studies that the availability of glucose is the rate-limiting step in glycolysis (24–26).

Recent data from the Chlamydia Genome Sequencing Project (http://chlamydia-www.berkeley.edu/4231/) has revealed the presence of several putative genes in *C. trachomatis* encoding proteins involved in energy metabolism, including enzymes in the glycolytic and tricarboxylic acid cycle pathways. Assuming that the genes express functional proteins, the chlamydiae could also contribute to the enhanced ATP levels observed during the infection. As the NMR technique cannot distinguish between ATP produced by the host cell and the bacteria, the metabolic changes could be due to both host and bacteria. Nonetheless, the overall ATP levels in the cell could not increase unless higher glucose concentrations became available, and thus both bacteria and host cells may benefit from the higher expression of host cell glucose transporters.

In agreement with previous studies demonstrating an ATP-ADP exchange activity in *C. psittaci* (8), the Chlamydia Genome Sequencing Project has also revealed the existence of a *Chlamydia* ADP/ATP translocase, which is homologous to the ADP/ATP translocase of another obligate intracellular bacterium, *Rickettsia prowazekii* (28). Although host-free RBs have low, short-lived metabolic activity, it was previously shown that isolated *C. psittaci* RBs, unlike the EBs, can in fact take up external ATP through an ATP-ADP exchange mechanism (8). The K_m for transport was approximately 5 μM, well below the eukaryotic ATP concentration of 1–5 mM. Thus, under the conditions of our *in vivo* measurements by NMR, all of the chlamydial transporters should have been functioning at V_{max}, their maximal rate. The requirement for plentiful supplies of host-cell ATP was also demonstrated by studies showing that the incorporation of exogenous glucose 6-phosphate, pyruvate, isoleucine, and aspartate into chlamydial proteins (29) and

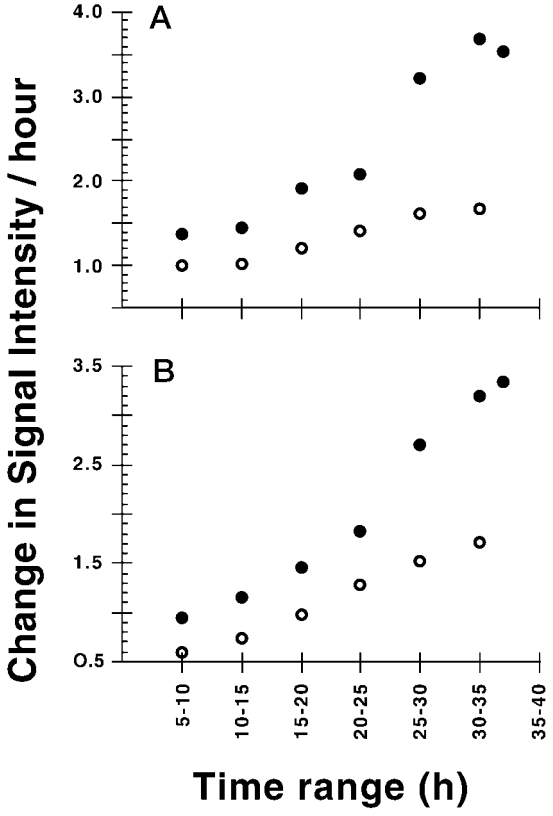

FIG. 6. **Rates of (*A*) glucose consumption and (*B*) lactate production in HeLa cells.** The levels of glucose and lactate were obtained from the ^{13}C spectra acquired on uninfected cells (○) ($n = 3$) or *Chlamydia*-infected cells (●) ($n = 2$). The rates were then determined for separate 5-h periods by calculating the relative slopes at which the intensity of the glucose peaks decreased and those of lactate increased. The slopes for the glucose intensities were then multiplied by −1.

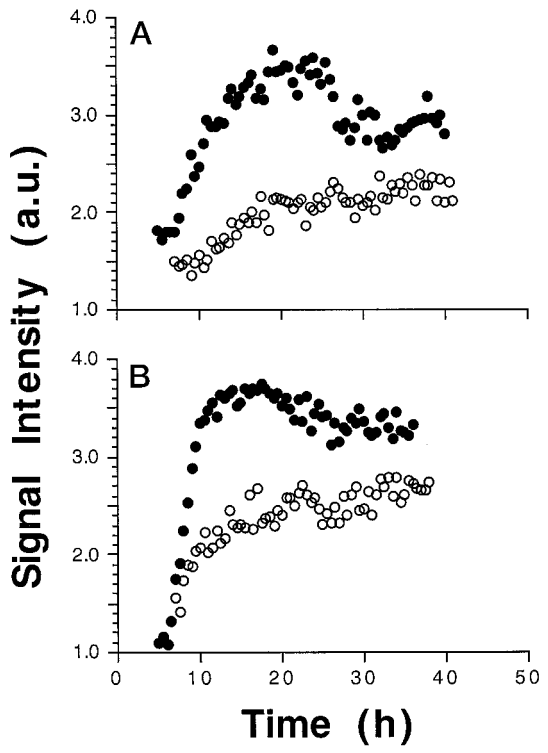

FIG. 7. **Relative concentrations of (*A*) glutamate and (*B*) glucose incorporated into glycogen studied as a function of time by noninvasive NMR.** ^{13}C spectra were acquired in uninfected cells (○) or *Chlamydia*-infected cells (●) as described under "Experimental Procedures."

bacterial synthesis of lipids and maintenance of the intrabacterial lysine pool (8, 29) also require exogenous ATP.

In contrast to our results, a recent study based on experiments with acid-soluble extracts of host cells found that NTP levels decreased in cells infected with chlamydiae (30). However, although we have used soluble extracts to assign the peaks in our NMR spectra with known standards, we have not attempted to use this invasive technique for following metabolite concentrations during the infection because of the inherent instability of the high-energy metabolites in the extracts and difficulties in quantitating the relative changes in metabolite concentrations in different extract preparations. Moreover, our noninvasive NMR measurements on living cells revealed an increase in the rate of glucose consumption midway through the infection cycle that agreed well with the glucose concentration changes that had been previously measured in the extracellular medium by standard chemical assays, which showed that infection of cells with *C. trachomatis* or *C. psittaci* increases the rate of consumption and catabolism of glucose (31–33).

The enhanced levels of energy metabolites in infected cells coincide with an increase in glucose consumption, which is most likely due to a *Chlamydia*-induced increase in the expression of glucose transporters on the surface of the infected cell. We have in fact observed that the expression of GLUT-1 increases by a factor of 2 in HeLa cells infected with *C. psittaci*.

GLUTs are a family of facilitated glucose transporters whose members have a high degree of sequence and structural homology among each other (27). GLUT-1 has an ubiquitous tissue distribution and is responsible for basal transport of glucose. Some transporters such as GLUT-4 are distributed primarily in adipose tissue and muscle and are localized almost exclusively in vesicles within the cell, while a substantial proportion of GLUT-1 is found on the plasma membrane (34, 35). The importance of GLUT-1 in energy metabolism *in vivo* has been shown by overexpressing the transporter in the muscle of transgenic mice, which led to enhanced glycolysis and increased levels of glycogen in the muscle (24, 36).

Insulin causes translocation of GLUT-4 from the internal vesicular pool to the plasma membrane, thus increasing cell surface levels of GLUT-4 by as much as 30-fold (27). However, GLUT-1 surface expression is increased only 2–3-fold by insulin (37), similar to the up-regulation induced by *Chlamydia* infection. Hence, the effects of *Chlamydia* infection on GLUT-1 levels in HeLa cells resembles the effects of insulin on GLUT-1 expression. It will now be worthwhile determining if other microbial infections representing an energy drain on the host also affect glucose transporter expression, and to elucidate the molecular basis for the increased expression.

In conclusion, our studies indicate that chlamydiae compensate for the extra energy load they represent on the infected cell by inducing an increase in the expression of glucose transporters in the host cell, which results in enhanced levels of high-energy metabolites in the infected cell. Thus, the bacteria have succeeded in ensuring an adequate supply of energy metabolites for themselves and for the survival of the host cell, at least long enough for the bacteria to undergo one complete infection cycle.

Acknowledgments—We are grateful to Véronique Colin and Philippe Souque for excellent technical assistance, Muriel Delepierre for help in the studies of cell extracts, Jean-Claude Bénichou and Valérie Imberti for help obtaining electron micrographs, and Richard Stephens (University of California, Berkeley) for communicating his genome data before publication.

REFERENCES

1. Paavonen, J., and Wolner-Hanssen, P. (1989) *Hum. Reprod.* **4,** 111–124
2. Jackson, L. A., and Grayston, J. T. (1996) *Curr. Opin. Infect. Dis.* **9,** 89–93
3. Moulder, J. W. (1991) *Microbiol. Rev.* **55,** 143–190
4. Hackstadt, T., Scidmore, M. A., and Rockey, D. D. (1995) *Proc. Natl. Acad. Sci. U. S. A.* **92,** 4877–4881
5. Rockey, D. D., Heinzen, R. A., and Hackstadt, T. (1995) *Mol. Microbiol.* **15,** 617–626
6. Perara, E., Yen, T. S., and Ganem, D. (1990) *Infect. Immun.* **58,** 3816–3818
7. Becker, Y. (1978) *Microbiol. Rev.* **42,** 274–306
8. Hatch, T. P., Al-Hossainy, E., and Silverman, J. A. (1982) *J. Bacteriol.* **150,** 662–670
9. Bavoil, P. M., Hsia, R.-c., and Rank, R. G. (1996) *Bull. Inst. Pasteur* **94,** 5–54
10. Batteiger, B. E., and Rank, R. G. (1987) *Infect. Immun.* **55,** 1767–1773
11. Neeman, M., Rushkin, E., Kadouri, A., and Degani, H. (1988) *Magn. Reson. Med.* **7,** 236–242
12. Degani, H., Ronen, S. M., and Furman-Haran, E. (1994) in *NMR in Physiology and Biomedicine* (Gillies, R. J., ed) pp. 329–351, Academic Press, San Diego
13. Tyagi, R. K., Azrad, A., Degani, H., and Salomon, Y. (1996) *Magn. Reson. Med.* **35,** 194–200
14. Ojcius, D. M., Niedergang, F., Subtil, A., Hellio, R., and Dautry-Varsat, A. (1996) *Res. Immunol.* **147,** 175–188
15. Raulston, J. E. (1997) *Infect. Immun.* **65,** 4539–4547
16. Schachter, J., and Wyrick, P. B. (1994) *Methods Enzymol.* **236,** 377–390
17. Evans, F. E., and Kaplan, N. O. (1977) *Proc. Natl. Acad. Sci. U. S. A.* **74,** 4909–4913
18. Navon, G., Navon, R., Shulman, R. G., and Yamane, T. (1978) *Proc. Natl. Acad. Sci. U. S. A.* **75,** 891–895
19. Gallis, J.-L., Delmas-Beauvieux, M.-C., Biran, M., Rousse, N., Durand, T., and Canioni, P. (1991) *NMR Biomed.* **4,** 279–285
20. Neeman, M., Eldar, H., Rushkin, E., and Degani, H. (1990) *Biochim. Biophys. Acta* **1052,** 255–263
21. Heinzen, R. A., Scidmore, M. A., Rockey, D. D., and Hackstadt, T. (1996) *Infect. Immun.* **64,** 769–809
22. Schramm, N., Bagnell, C. R., and Wyrick, P. B. (1996) *Infect. Immun.* **64,** 1208–1214
23. Shedd, S. F., Lutz, N. W., and Hull, W. E. (1993) *NMR Biomed.* **6,** 254–263
24. Ren, J.-M., Marshall, B. A., Gulve, E. A., Gao, J., Johnson, D. W., Holloszy, J. O., and Mueckler, M. (1993) *J. Biol. Chem.* **268,** 16113–16115
25. Bissell, M. J. (1976) *J. Cell. Physiol.* **89,** 701–709
26. Dominguez, J. H., Song, B., Liu-Chen, S., Qulali, M., Howard, R., Lee, C. H., and McAteer, J. (1996) *J. Clin. Invest.* **98,** 395–404
27. James, D. E., Piper, R. C., and Slot, J. W. (1993) *J. Cell Sci.* **104,** 607–612
28. Winkler, H. H. (1990) *Annu. Rev. Microbiol.* **44,** 131–153
29. Weiss, E., and Wilson, N. N. (1969) *J. Bacteriol.* **97,** 719–724
30. Tipples, G., and McClarty, G. (1993) *Mol. Microbiol.* **8,** 1105–1114
31. Gill, S. D., and Stewart, R. B. (1970) *Can. J. Microbiol.* **16,** 997–1001
32. Moulder, J. W. (1970) *J. Bacteriol.* **104,** 1189–1196
33. Mavrov, I. I., Goncharenko, M. S., Shchegoleva, E. V., Chernobaeva, I. A., and Pustovoitova, L. M. (1991) *Mikrobiol. Zh.* (*Kiev*) **53,** 95–98
34. Hudson, A. W., Ruiz, M., and Birnbaum, M. J. (1992) *J. Cell Biol.* **116,** 785–797
35. Haney, P. M., Slot, J. W., Piper, R. C., James, D. E., and Mueckler, M. (1991) *J. Cell Biol.* **114,** 689–699
36. Marshall, B. A., Ren, J.-M., Johnson, D. W., Gibbs, E. M., Lillquist, J. S., Soeller, W. C., Holloszy, J. O., and Mueckler, M. (1993) *J. Biol. Chem.* **268,** 18442–18445
37. Piper, R. C., Hess, L. J., and James, D. E. (1991) *Am. J. Physiol.* **260,** C570–C580